Investigation of Ablation Techniques for Different Types of Brain Tumors

Author

MANAHIL BINTE IRFAN

MS-BME-17, 204657

Supervisor

Dr. SYED OMER GILANI

DEPARTMENT OF BIOMEDICAL ENGINEERING & SCIENCES

SCHOOL OF MECHANICAL & MANUFACTURING ENGINEERING

NATIONAL UNIVERSITY OF SCIENCES AND TECHNOLOGY

ISLAMABAD

MAY 2021

Investigation of Ablation Techniques for Different Types of Brain Tumors

Author

MANAHIL BINTE IRFAN

Regn Number

MS-BME-17, 204657

A thesis submitted in partial fulfillment of the requirements for the degree of

MS Biomedical Engineering

Thesis Supervisor:

Dr. SYED OMER GILANI

Thesis Supervisor's Signature: _____

DEPARTMENT OF BIOMEDICAL ENGINEERING & SCIENCES
SCHOOL OF MECHANICAL & MANUFACTURING ENGINEERING
NATIONAL UNIVERSITY OF SCIENCES AND TECHNOLOGY,
ISLAMABAD

MAY 2021

MASTER THESIS WORK

We hereby recommend that the dissertation prepared under our supervision by: **Manahil Binte Irfan** (**MS-BME-17, 204657)** Titled: **Investigation of Ablation Techniques for Different Types of Brain Tumors** be accepted in partial fulfillment of the requirements for the award of _____degree.

Examination Committee Members

1. Name: Dr. Aamir Mubashar Signature: _____

2. Name: Dr. Emad ud Din Signature: _____

3. Name: Dr. Asim Waris Signature: _____

Supervisor's name: Dr. Syed Omer Gilani Signature: _____

Date: _____

_____ _____

Head of Department Date

COUNTERSIGNED

Date: _____

_____

Dean/Principal

Thesis Acceptance Certificate

It is certified that the final copy of MS Thesis written by **Manahil Binte Irfan** (Registration No. 204657), of SMME (School of Mechanical & Manufacturing Engineering) has been vetted by undersigned, found complete in all respects as per NUST statutes / regulations, is free of plagiarism, errors and mistakes and is accepted as partial fulfilment for award of MS/MPhil Degree. It is further certified that necessary amendments as pointed out by GEC members of the scholar have also been incorporated in this dissertation.

Signature:_____

Supervisor: Dr. Syed Omer Gilani

Date:_____

Signature (HOD):_____

Date:_____

Signature (Principal):_____

Date:_____

Declaration

I certify that this research work titled "*Investigation of Ablation Techniques for Different Types of Brain Tumors"* is my own work. The work has not been presented elsewhere for assessment. The material that has been used from other sources has been properly acknowledged / referred.

Signature of Student

Manahil Binte Irfan

MS-BME-17, 204657

Plagiarism Certificate (Turnitin Report)

This thesis has been checked for Plagiarism. Turnitin report endorsed by Supervisor is attached.

Signature of Student
Manahil Binte Irfan
MS-BME-17, 204657

Signature of Supervisor

Proposed Certificate for Plagiarism

It is certified that PhD/M.Phil/MS Thesis Titled **Investigation of Ablation Techniques for Different Types of Brain Tumors** by **Manahil Binte Irfan** has been examined by us. We undertake the follows:

a. Thesis has significant new work/knowledge as compared already published or are under consideration to be published elsewhere. No sentence, equation, diagram, table, paragraph or section has been copied verbatim from previous work unless it is placed under quotation marks and duly referenced.
b. The work presented is original and own work of the author (i.e. there is no plagiarism). No ideas, processes, results or words of others have been presented as Author own work.
c. There is no fabrication of data or results which have been compiled/analyzed.
d. There is no falsification by manipulating research materials, equipment or processes, or changing or omitting data or results such that the research is not accurately represented in the research record.
e. The thesis has been checked using TURNITIN (copy of originality report attached) and found within limits as per HEC plagiarism Policy and instructions issued from time to time.

Name & Signature of Supervisor

Dr. Syed Omer Gilani

Copyright Statement

- Copyright in text of this thesis rests with the student author. Copies (by any process) either in full, or of extracts, may be made only in accordance with instructions given by the author and lodged in the Library of NUST School of Mechanical & Manufacturing Engineering (SMME). Details may be obtained by the Librarian. This page must form part of any such copies made. Further copies (by any process) may not be made without the permission (in writing) of the author.
- The ownership of any intellectual property rights which may be described in this thesis is vested in NUST School of Mechanical & Manufacturing Engineering, subject to any prior agreement to the contrary, and may not be made available for use by third parties without the written permission of the SMME, which will prescribe the terms and conditions of any such agreement.
- Further information on the conditions under which disclosures and exploitation may take place is available from the Library of NUST School of Mechanical & Manufacturing Engineering, Islamabad.

Acknowledgements

First and foremost, praises and thanks to Allah, the Almighty, for His showers of blessings throughout my research work to complete it successfully just in time.

I am extremely grateful to my parents, Dr. Muhammad Irfan and Dr. Mussarrat Jabeen, for their love, prayers, and care. Their dynamism, vision, sincerity and motivation has kept me going. I express my thanks to my sister and brother for their support and invaluable prayers, and their constant nagging which eventually got the job done. I am very much thankful to my husband for his love, understanding, prayers and continuing support to complete this research thesis.

I would like to express my deep and sincere gratitude to my research supervisor and co-supervisor, Dr. Syed Omer Gilani and Dr. Aamir Mubashar respectively, for giving me the opportunity to do research and providing invaluable guidance throughout this research. They have taught me the methodology to carry out research and to present the research works as clearly as possible. It was a great privilege and honor to work and study under their guidance.

Special thanks to my girls, Fifi, Fajar, Zara, and Naveed e Saba, the four best people to have found me in this world. For always being there for me. Nudging and probing me to get to work, helping me through my depression spells, really empathizing with me and making me look at things in a different, broader view but most of all, for believing in me. I cannot thank you enough. God be with you. I am extremely grateful for what you lot have offered me. Thank you for your friendship and your great sense of humor. Thank you for being patient with me!

Dedicated to my beloved parents, adored siblings, and kind husband whose tremendous support and cooperation led me to this wonderful accomplishment.

Abstract

The main goal of treatment of intracranial neoplasms is to eradicate tumor cells with minimal disruption of surrounding normal parenchyma. Stereotactic radiosurgery (SRS) has been used as one modality of treatment in appropriate cases. SRS is limited by the dose a patient can tolerate and adverse effects of radiation. These limitations provide a niche for alternative therapies. Furthermore, tissue samples cannot be obtained during treatment. Recently, thermal therapies including high-intensity focused ultrasound (HIFU) and laser interstitial thermal therapy (LITT) have been proposed as alternatives. The purpose of this study is to develop simplified 3D models of different types of brain tumors from MRI scans, investigate different ablation techniques for removal of such tumor, and optimize these techniques for different locations, sizes, and types of tumors.

With the vast advancements in medical devices technology, brain tumors have become increasingly viable to cure through surgery and/or adjuvant noninvasive therapies. The choice of the treatment plan is highly dependent on the location of the tumor. Tumors located deep in the parenchyma of the brain can only be treated by ablative techniques and therefore, thorough investigation of techniques like High Intensity Focused Ultrasound (HIFU) and Laser Interstitial Thermal Therapy (LITT) is imperative. In this study, HIFU and LITT have been investigated and compared under four simulative environments in COMSOL Multiphysics which also accommodate the possibility of the presence of an artery or an organ near tumor site. It has been found out that HIFU is more focally contained compared to LITT. LITT causes more irreversible damage to the tumor compared to HIFU. Both the techniques resulted in damage to nearby artery, but the damage caused by HIFU was less compared to that caused by LITT.

Key Words: *High Intensity focused Ultrasound, Laser Interstitial Thermal Therapy, Ablation, Tumor reduction, Arrhenius Law*

Table of Contents

List of Figures

List of Tables

CHAPTER 1: INTRODUCTION

The research work in this thesis is laid out as follows: Introduction discusses the previous simulative work done in HIFU therapy and LITT and defines the need of this research. Methodology section explains the four case studies in detail namely, artery in the path of HIFU beam, artery away from the HIFU beam, artery 1.5 mm away from the LITT focal point, and artery 3 mm away from LITT focal point. Results section declares and discusses the findings of this research and conclusion presents the conclusive remarks of the paper and notes on future works.

1.1 Background, Scope and Motivation

Brain tumors are excessive growth of abnormal cells in the brain, mainly categorized as malignant or benign tumors. Prevalence estimates depict a gradual increment in brain tumor patients through the years. In the years 1985 - 1989, 97.5 per 100,000 persons were diagnosed with brain tumors [1]. This number doubled to 221.8 per 100,000 in a span of 20 years [1]. In 2015, 22,850 U.S. individuals were diagnosed with brain tumors out of which approximately 15,320 cases resulted in death [2]. Brain tumors occur along the entire age spectrum, with a significant reduction in survival rates as the age bracket increases [3]. Although most common in adults, brain tumors have a fair representation in pediatric oncology as well.

Tumor morphology, such as its size, histology, and location, determine the context for the choice of appropriate treatment for a given tumor [4]. Until recently, brain tumors have been predominantly treated with the golden practice of Surgery, Whole-Brain Radiation Therapy (WBRT), Chemotherapy, and Stereotactic Radiosurgery (SRS) [5]–[8]. Surgical resection is useful for treating benign tumors with a single metastatic lesion in a non-eloquent cortex [4] and therefore, most benign tumors can be successfully excised via the process. However, malignant tumor surgery only provides symptomatic relief by reducing the raised intracranial pressure [9]. Histological heterogeneity of malignant tumor cases such as Glioblastoma Multiforme (GBM) deems complete eradication impossible [10]. In such cases, WBRT is used in conjunction with surgery to reduce recurrence rates [11]. However, radiation deforms both tumor cells and the normal brain [12]. Thus, radiation necrosis and leukoencephalopathy are concomitant with this

procedure[13], [14]. Therefore, any potential consequences must be weighed in with the benefits before opting for this procedure.

Advances have been made in the past decade for local chemotherapy delivery, but they come with myriad limitations such as reduced drug penetration, unpredictable distribution, elevated intracranial pressures, and long infusion times [15]. Lastly, SRS is only fully effective in treating primary glial tumors. In the case of GBM, which commonly infiltrates the brain parenchyma, SRS is only helpful as a salvage treatment after primary surgery, or WBRT has been performed to contain glioma tumors to some extent [16]. Although SRS significantly reduces exposure to ionizing radiation by pointedly targeting tumor cells and obviating the normal surrounding cells, 84% of postoperative cases still develop leukoencephalopathy within 4 years [14].

The invasive and adverse nature of these techniques, sometimes resulting in debilitating concomitants or disqualification of patients from treatments altogether, has motivated research toward alternative therapies. Recently, there has been growing appeal for thermal therapies such as High-Intensity Focused Ultrasound (HIFU) and Laser Interstitial Thermal Therapy (LITT)[17]. HIFU and LITT have been aptly applied to treat essential tremors and epilepsy, respectively[18]– [20]. These two thermal therapies have a similar workflow, but the production and origin of the thermal energy vary, as does energy distribution. They prove most beneficial when treating a deep-seated, focally- contained lesion in the parenchyma, which is otherwise inapproachable through surgery [4]. Noninvasive HIFU used as primary therapy and palliative care represents a significant improvement in patient safety and survival in initial studies [21], [22]. Although invasive, LITT requires less healing period and speeds up adjuvant treatments such as chemotherapy and radiation therapy [4].

1.1.1 High Intensity Focused Ultrasound

The physics of HIFU is based on ultrasound wave propagation through a medium of intervening tissue to a target ablative region. It increases the temperature of a specific point or brings about other biological changes in a noninvasive manner. Because of its noninvasive

property, this therapy has caught the attention of scientists and physicians alike in hopes of building a complication-free intervention tool.

Recent experimental developments have revealed that when one lung is flooded, it invokes its atypical acoustic nature as a saline tissue, providing access to central lung tumors through HIFU. In [23], an ultrasound simulation tool and a bioheat solver were made in MATLAB environment to predict HIFU induced heating congruent with ablation regions over time. It was discovered that heat induction and the size of the lesion were improved due to low attenuation in the flooded lung. The raster scheme was recommended for benign lung tumors, while the volumetric scheme was deemed suitable for malignant tumors. It was observed that in one flooding session, 3 cm tumors could be effectively ablated within a 3mm margin. While beneficial for HIFU implementation, the acoustic conditions of the flooded lung required customized therapy planning.

HIFU has also been used to precipitate Deep Vein Thrombosis (DVT) of the iliofemoral veins. However, damage to surrounding tissue or veins has been observed in all previous studies. In their simulation [24], Smirnov et al. used a phased array device instead of a single transducer to reduce the transducer's otherwise large focal region. Different geometries of the array were considered to figure out the optimum geometric configuration of the array. It was determined in the simulation model that 7680 elements placed at $\lambda/2$ distance from each other to form a cylindrical array with each element operating at a frequency of 500 kHz reduced the lesion zone within the femoral vein considerably. This study also depicted that an efficient array comprising fewer elements operating at lower frequencies could be built.

HIFU array has also been used to treat tumors in the thoracic region enveloped by ribs. Ribs hinder the HIFU therapy because they absorb the beam energy, which in turn raises the temperature of the ribs. Consequently, the beam and the HIFU temperature field get distorted. These challenges were addressed in a research investigation [25] wherein a refocusing algorithm called Limited Power Deposition (LPD) was developed, which limited the power accumulation in the ribs and focused maximum energy at the tumor zone. In [26], an Iterative Sparse Limited Power Deposition (ISLPD) was numerically simulated that utilized a smaller number of elements within a transducer array for HIFU while maintaining focal heating comparable to that in

previous techniques. It was achieved by running multiple sets of sparsity solutions and removing any least utilized elements in the previous runs. The remaining elements could be used for concurrent processes such as motion tracking and imaging. Wave propagation and temperature profiles were simulated to illustrate the advantages of this approach.

In most previous simulative studies, it was assumed that tissue properties do not change over time when HIFU is applied to a morbid tissue for the sake of smooth simulations and rudimentary results. However, the fact remains that whenever high temperature is applied to a focal region, it causes a temperature rise in the surrounding tissue, which in turn affects the temperature and acoustic fields of HIFU. In their numerical simulation [27], Tan Q et al. present an acoustic-thermal coupling model to predict the temperature distribution and tissue necrosis via the Westervelt equation and Pennes' bioheat transfer equation. They also considered the isolated impact and the combined effect of all tissue properties. The results represented that acoustic absorption had the most impact of temperature and thermal necrosis amongst all dynamic tissue properties. Additionally, the acoustic absorption coefficient also contributed to elevated temperature in the focal region and a broader tissue damage region. Conversely, blood perfusion led to a lower temperature in the focal region and a smaller necrosis region than the other simulations performed using the rest of the dynamic tissue properties.

Based on a similar premise as the study mentioned above, another research [28] was carried out to increase the HIFU beam energy and focal region and reduce sonification time to minimize the cooling effect of blood circulation in the morbid tissue. A dual-concentric HIFU transducer run by multiple phase-inverted frequencies was proposed. It considerably expanded the focal region and reduced the notch point level formed between the two lobes whenever dual-concentric geometry was used. The transducer acoustic field, electrical impedance, and impulse response were simulated to examine the proposed transducer's efficacy. A bioheat transfer model was simulated to investigate the lesion volume. The results showed potential because the proposed method cultivated a 141% increase in lesion size compared to a single element transducer, thus reducing the therapy's total treatment time.

Similarly, reference [29] investigated blood vessels' role in the HIFU therapy temperature profile during liver tumor ablation. A 3D acoustics-thermal coupling model simulated the

temperature distribution in the hepatic carcinoma zone. The hepatic vessels and parenchyma were modeled in linear Westervelt and Pennes' equations and nonlinear Navier- Stokes' equations. Acoustic streaming was also included in the simulation. It was ascertained that acoustic streaming and convective cooling in large blood vessels contributed significantly to the temperature profile and lesion zone near vessels.

Another reference [30] researched nonlinear propagation effects on the HIFU temperature distribution via the nonlinear Westervelt equation and Pennes' bioheat equation. Weak effects were also taken into account. Correlation between measured and predicted temperature profiles and lesion sizes in the porcine muscle were studied. An acoustic power of 24-56 W was applied on the porcine muscle for 30 s. It was established that the measured and predicted temperature elevations correlated for temperatures below 85-90 °C. Temperatures above 85-90 °C resulted in cavitation, thence distorting the lesion zone and causing the simulated temperature to deviate from the measured temperature.

1.1.2 Laser Interstitial Thermal Therapy

LITT therapy works on the principle of light absorption which releases thermal energy from low voltage laser. This procedure increases the temperature at the tip of the laser probe and results in liquefactive ablation. Although invasive, studies depict minimal complications and increased survival rate in patients with recurrent GBM [31]. However, it cannot be used near large vessels, or hemorrhages [31], [32].

In [33], a simple LITT model was mathematically simulated to assist physicians in thoroughly planning thermal treatment doses to optimize therapeutic effects of the procedure while curtailing any side effects occurring because of ill planning and management. The brain was simulated as seven compartments (A, B, C, E, V, S, F) illustrating the blood flow and the Cerebrospinal Fluid (CSF) flow. Four analyses were run on the model to check its robustness, namely, mechanical analysis, fluid dynamics, bioheat transfer, and laser beam. It was simulated such that LITT was applied to the brain model for 1 s, and the temperature was kept within the range of 50 °C – 90 °C. It was shown that LITT desiccated and ablated the tumor cells present within the brain tissue.

When thermal ablation is applied, the dynamic brain tissue properties render post-treatment effects of LITT unpredictable and limit its utility. A single-blind study [34] utilized the Arrhenius model to calculate the Thermal Damage Estimate (TDE), which evaluates the extent of tissue necrosis after ablation. The Medtronic Visualase console maintained a dataset of 22 cases by providing post-therapy enhanced axial images and intraoperative TDE images of each patient. The cross-sectional ablation area of the enhanced images and necrosis area for the TDE images were calculated and tested for correlation. Two blinded raters determined a strong correlation between the experimental lesion zone and measured TDE hence proving TDE an accurate measure of lesion size caused by LITT in a human brain.

Similar to the previous study, in [35], intraoperative TDE maps and pre-, intra- and postoperative MRIs of the mesial temporal lobe of 30 patients with Mesial Temporal Epilepsy (MLE) treated with LITT were utilized to study short- and long-term effects of the laser therapy. Any preoperative independent variables that could affect the process were also studied. The overlap among the TDE maps and immediate post ablative and delayed ablative zones were calculated using Dice Similarity Coefficient (DSC). Moreover, ablative dynamics and thermal time constant τ of the amygdala and hippocampal head tissue were estimated using the first-order linear bioheat transfer model. These dynamics were then compared to 16 independent variables acquired from patient demographics, mesial temporal anatomy, and pre-, intra- and postoperative imaging characteristics. It was determined that TDE maps correlated with immediate ablative zones but were notably more massive than the delayed LITT effects, specifically at the amygdala and hippocampal head. TDE maps predicted accurately for delayed ablative zones in cases with smaller peri hippocampal CSF spaces. This study depicted that patient demographics, the medial temporal lobe anatomy, and pathology may control ablative tissue effects.

HIFU and LITT have been thoroughly investigated individually in previous papers but none of the papers compare them side-by-side under different simulated environments. In this paper, four case studies involving HIFU and LITT have been simulated and analyzed to compare the precision of both ablative techniques, their respective effects on the tumor site and to evaluate the thermal damage caused by these techniques to an artery placed close to the tumor. The position of the artery has been varied in the case studies. This research not only aims at

honing better insight into the fundamental working of these techniques but also in aiding physicians to develop accurate clinical protocols for the treatment plan of these ablative techniques, depending on the placement of the brain tumor and neighboring organs.

CHAPTER 2: METHODOLOGY

This research focuses on the comparative study of high intensity focused ultrasound (HIFU) and laser interstitial thermal therapy (LITT). The techniques were compared with numerical models developed using finite element method.

2.1 Software

The numerical simulation models were developed in commercial finite element code COMSOL Multiphysics that is capable of handling multiphysics problems by providing coupling between various fields. Simulation of the selected techniques involved pressure acoustics field and laser heat source, and their interaction with bio-matter resulting in bioheat transfer.

2.2 Ablation Techniques

Both HIFU and LITT were employed to destroy a representative tumor in brain matter by ablation. A neighboring artery was also placed at different locations with respect to the tumor to compare the effects of both the techniques on the artery. Four case studies were carried out with the developed simulation models and the results were compared to provide a comparison of the two selected techniques. In this research study, cranium was not included in any numerical models.

2.2.1 High Intensity Focused Ultrasound

In the HIFU simulation model, the pressure acoustic field was solved to determine the temperature increase in the tumor caused by a beam of focused ultrasound. The governing equation of the pressure acoustic field was Helmholtz equation based on the assumptions that the ultrasound wave propagation was linear and the amplitude of shear waves was insignificant compared to the amplitude of acoustic pressure waves. The Helmholtz equation is given in Eq (2.1).

$$\frac{\partial}{\partial r}\left[-\frac{r}{\rho_c}\left(\frac{\partial p}{\partial r}\right)\right]+r\frac{\partial}{\partial z}\left[-\frac{1}{\rho_c}\left(\frac{\partial p}{\partial z}\right)\right]-\left[\left(\frac{\omega}{c_c}\right)^2\right]\frac{rp}{\rho_c}=0 \quad (2.1)$$

where r is radial coordinate, z is axial coordinate, p is acoustic pressure, ω is angular frequency, ρ_c is complex density and c_c is complex speed of sound. ρ_c and c_c incorporate the damping properties of the material.

Coupling medium was assumed lossless and the case study models aptly simulated tissue heating during HIFU therapy provided the acoustic pressure at the focal point was well below acoustic cavitation threshold. Given the acoustic pressure field, acoustic intensity field and heat source Q, the tissue heating was calculated with the Pennes' Bioheat Transfer equation given below;

$$\rho C_p\frac{\partial T}{\partial t}=\nabla.(k\nabla T)-\rho_b C_b w_b\,(T-T_b)+Q+Q_{met} \quad (2.2)$$

where T is temperature of the tissue, ρ is density of the brain tissue, C_p is brain tissue specific heat, k is thermal conductivity, ρ_b is blood density, C_b is blood specific heat, w_b is blood perfusion rate, T_b is blood temperature, Q is heat source, and Q_{met} is metabolic heat source. Q_{met} was not included in this study.

2.2.2 Laser Interstitial Thermal Therapy

The laser-induced tissue ablation in the LITT simulation model and the temperature profile of the irradiated tumor were modelled by Eq (2.2). The heat source Q in Eq (2.2) depicts the laser-tissue interaction and was modelled using Beer-Lambert Law under the assumption that the emitted light comprised a single wavelength and was parallel. The Beer-Lambert law is given as;

$$\frac{\partial I}{\partial y}=\alpha(T)*I \quad (2.3)$$

where $\frac{\partial I}{\partial y}$ is the differential form of light intensity along the laser beam direction which is also the heat source Q in this scenario and α(T) is temperature dependent light absorption coefficient of the tissue. It was assumed that the emitted light refracted, reflected, or scattered

minimally inside the brain tissue. Tissue was assumed to be homogenous and isotropic. The incident laser beam propagated from the origin following a Gaussian profile.

2.3 Case Studies

2.3.1 Artery in the path of HIFU beam

The 2D-axisymmetric geometry to model High Intensity Focused Ultrasound in a scenario wherein artery lay in the path of the beam was developed, as shown in Figure 2.1. The model geometry comprised an acoustic transducer, coupling medium, brain tissue, artery, and tumor. The concave transducer was 10 mm in radius with a focal length of 17 mm, and a thickness of 3 mm. The cylindrical tissue was 40 mm in length, and a 1 mm layer of coupling medium existed between the brain tissue and transducer. An artery of 3 mm diameter was simulated in the path of the HIFU beam to test the effect of focused ultrasound beam on the artery. The transducer and brain tissue were arranged coaxially. Hence, the model was developed as 2D-axisymmetric. An ellipse was made at the focal region of the transducer to depict tumor tissue. The ellipse dimensions were 2.5 mm a semi-axis and 0.65 mm b semi-axis to accommodate a finer mesh in this area compared to the rest of the geometry to incorporate the sharp acoustic and heat gradients here. Perfectly Matched Layers (PMLs) of width 3 mm were introduced on the top and right side of the brain tissue and the right side of the medium to absorb outgoing waves and simulate linear wave propagation while neglecting shear waves.

The HIFU transducer was operated for 1 s at a frequency of 1.965 MHz and then turned off to allow the tissue to cool down to its surrounding temperature of 310.05K [37]. A step function was defined to model this heating and cooling phenomenon. Water was used as the coupling medium in these case studies. The properties of water were defined as per COMSOL library. The material properties of the rest of the layers were defined as listed in Tables 2.1 and 2.2. Pressure Acoustics, Frequency Domain (*acpr*) module was run on the entire geometry while Bioheat Transfer was only run on the brain tissue. Pressure Acoustics was defined separately for water, tissue, and artery domain to simulate their respective absorption coefficients. The temperature of tissue and artery domains was set at 310.05K while the temperature of the transducer and the coupling medium was set at 300.15 K. The displacement amplitude of the transducer was defined.

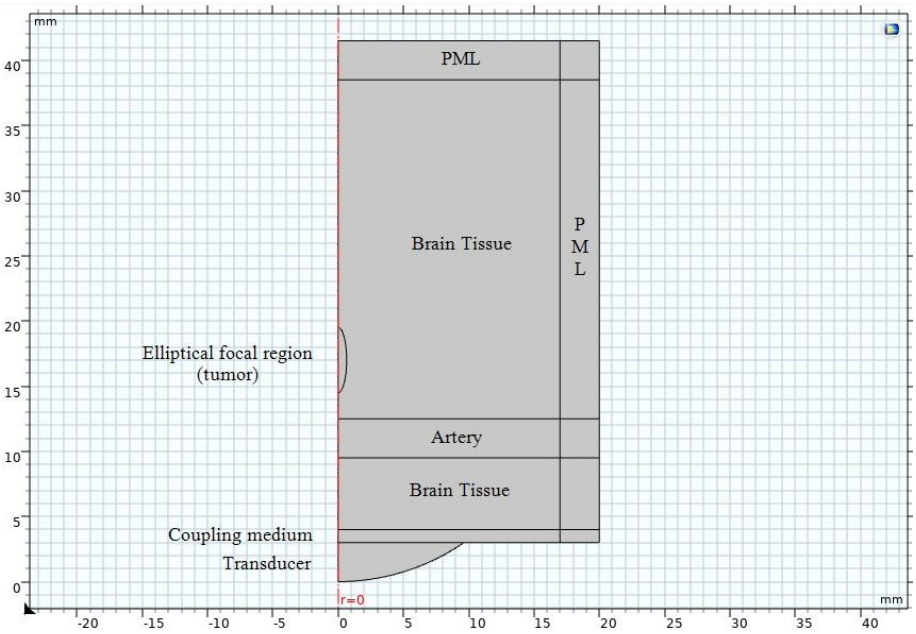

Fig 2.1: 2D axisymmetric model of artery lying in the path of the ultrasound beam

For bioheat transfer, the entire brain tissue served as a heat source. Q_0 was calculated while running Pressure Acoustics, Frequency domain study. Bioheat transfer was defined separately for brain tissue and artery domain to simulate their different material properties such as density, thermal conductivity, and heat capacity. The inner borders of the tissue domain were set to 310.05K.

Two separate meshes were made for each module. For Pressure Acoustics, Frequency Domain, the entire geometry was meshed at $\lambda/5$ in free triangular elements save for the elliptic region and the artery which were finely meshed at $\lambda/8$. A mapped rectangular mesh was laid in the top and cylindrical PMLs to account for anisotropy without compromising the quality of the mesh even if each element had more degrees of freedom. A coarser and localized mesh in the brain tissue was made for Bioheat Transfer module with a fine mesh of $\lambda/8$ at the focal region and the artery.

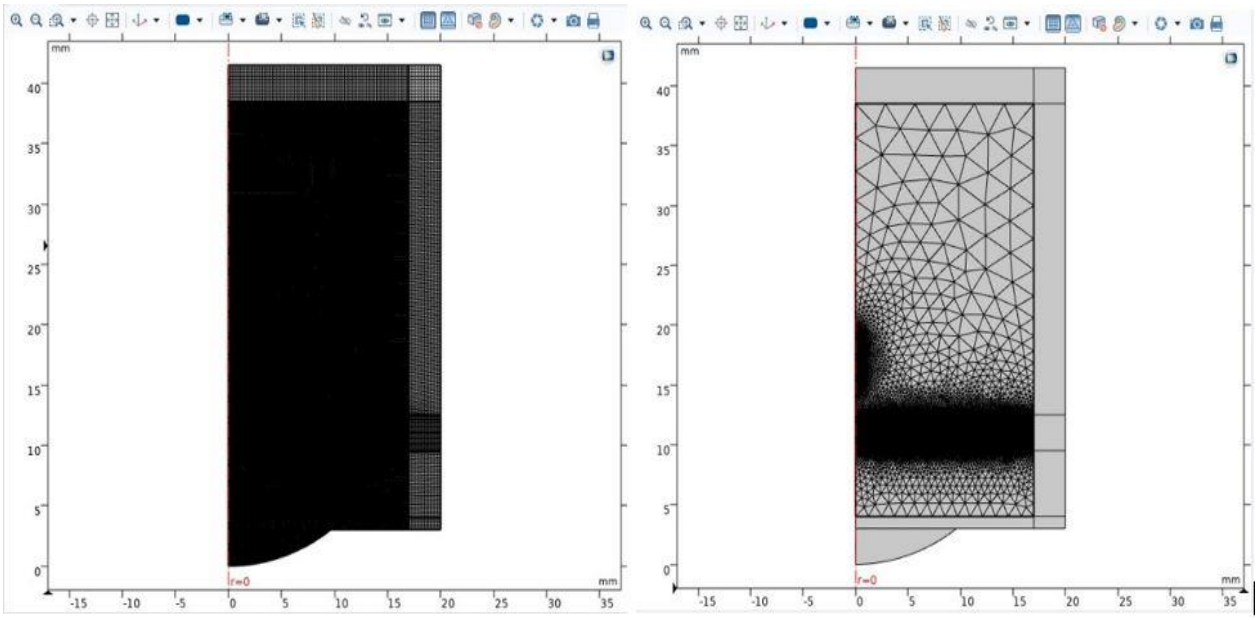

Fig. 2.2: Complete mesh of Pressure Acoustics module with finer focal region and artery, and precisely mapped rectangular border meshes (left),
Localized mesh for Bioheat transfer module (right)

2.3.2 Artery away from the path of HIFU beam

For the scenario where the artery lay away from the HIFU beam, the orientation, and parameters of the HIFU model were identical as mentioned in the previous study with the only difference lying in the position of the artery, as depicted in Figure 2.3.

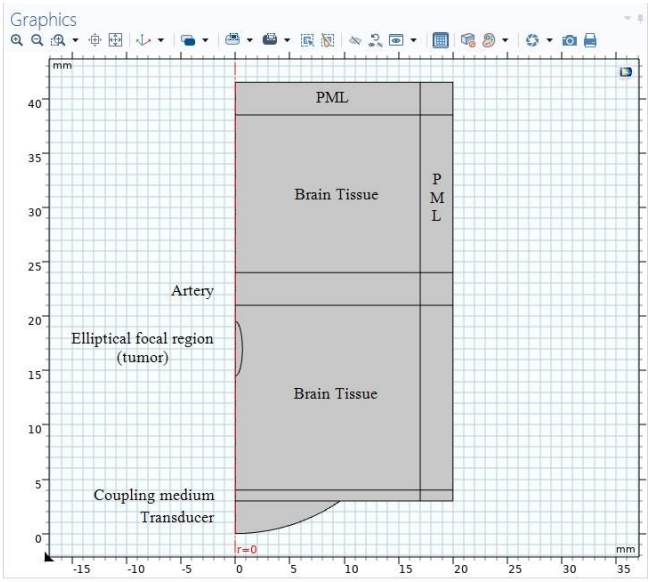

Fig. 2.1: 2D axisymmetric model of artery lying away from the path of the HIFU beam.

2.3.3 Artery at a distance of 1.5mm from the LITT focal point

In case of LITT, the 2D-axisymmetric model was developed, as shown in Figure 2.4. The model geometry comprised brain tissue, artery, tumor, and a laser probe. The diffuse-tip catheter was 1.65 mm in radius. The tip of the catheter was placed in the middle of the tumor. The geometry of brain tissue and artery was similar to that in HIFU case studies with the absence of coupling medium and acoustic transducer. In this scenario, the artery was placed at 1.5 mm from the tumor region.

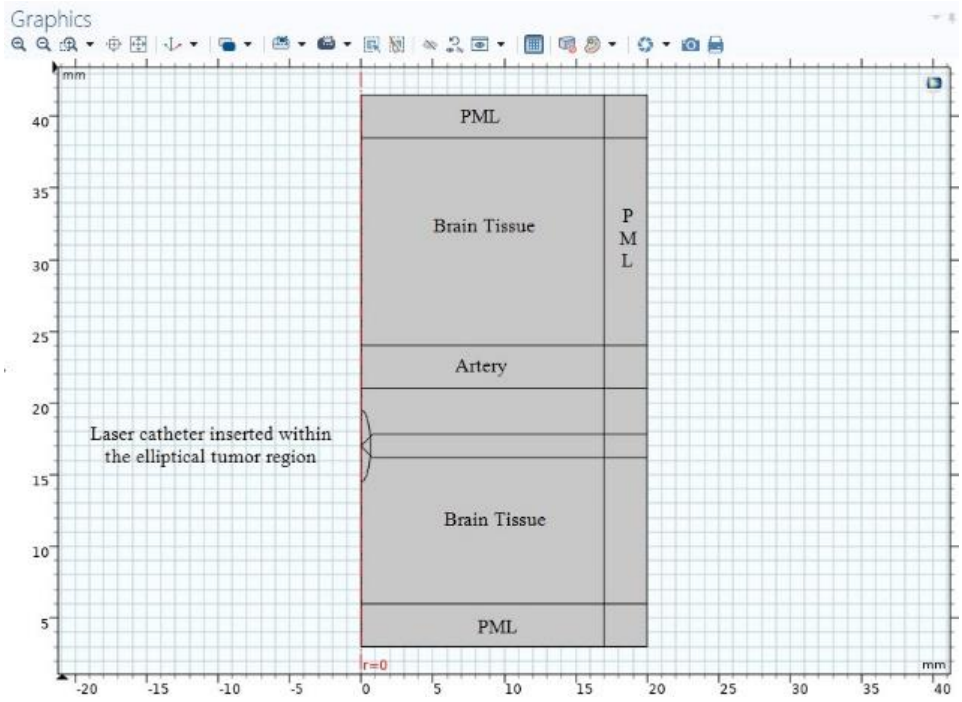

Fig. 2.4: 2D axisymmetric model of artery lying 1.5mm away from LITT focal point

Bioheat transfer was defined separately for brain tissue and artery domain to simulate their different material properties such as density, thermal conductivity, and heat capacity. The material properties of the probe were defined as per COMSOL library as fused silica. Beer-Lambert Law (2.3) was implemented and solved in COMSOL as a partial differential equation. A zero-flux boundary condition was introduced on all the boundaries (except the illuminated one) of the geometry depicting that any light reaching these boundaries would leave the domain. Laser intensity at the origin of the catheter was 3 W/mm^2 with a spot radius of 2 mm. It was delivered continually for 20 s. This was implemented in the geometry as a Dirichlet boundary

condition at the catheter tip, where it made contact with the tissue. The entire geometry was finely meshed as shown in the Figure 2.5.

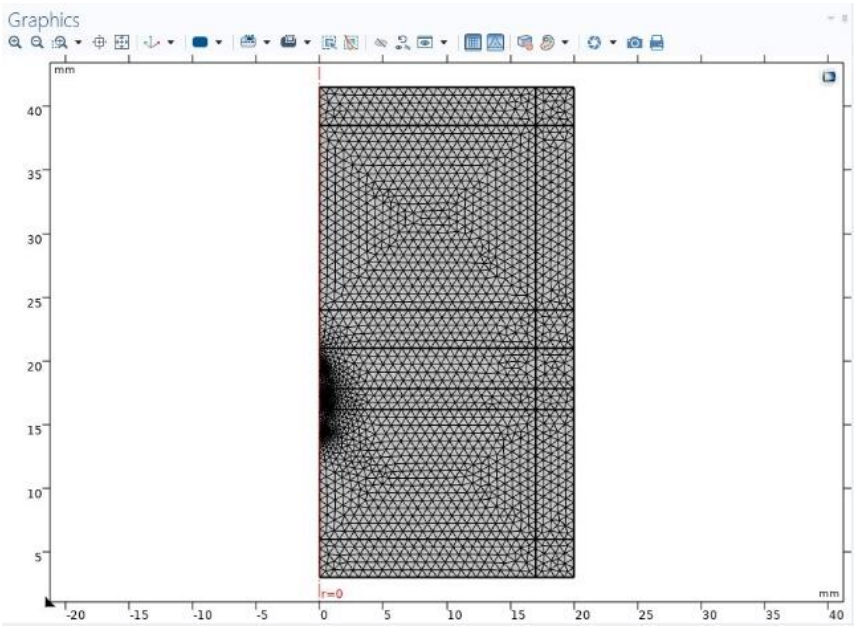

Fig. 2.5: Complete fine mesh of the LITT geometry

2.3.4 Artery at a distance of 1.5mm from the LITT focal point

Another LITT simulation was made wherein the artery lay 3mm away from the LITT focal point as shown in Figure 2.6. In this case, the orientation, and parameters of the LITT model were identical as mentioned in the previous study with the only difference lying in the distance of the artery from the tumor site.

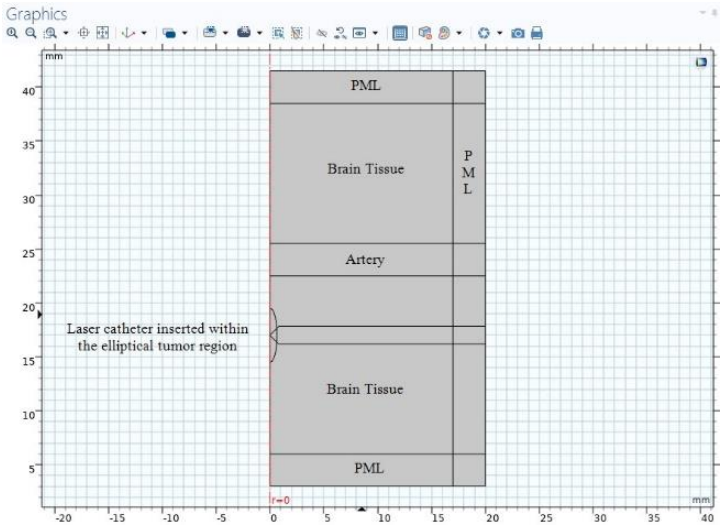

Fig. 2.6: 2D axisymmetric model of artery lying 3mm away from tumor region

2.4 Damage Integral

For all the case studies, damage integral was utilized to compute the fraction of necrotic tissue and neighboring artery. The degree of tissue damage α was evaluated by Arrhenius eq (2.4);

$$\frac{\partial \alpha}{\partial t} = (1-\alpha)^n A e^{\frac{\Delta E}{RT}} \quad (2.4)$$

Where A is the frequency factor, ΔE is the activation energy required to induce irreversible damage to the tissue, and R is the universal gas constant. The values for the parameters are tabulated in Table (3). The fraction of necrotic tissue was then determined as Eq (5);

$$\theta_d = \min\left(\max(\alpha, 0), 1\right) \quad (2.5)$$

CHAPTER 3: RESULTS AND DISCUSSION

Three aspects of the ablation techniques were scrutinized in the four case studies mentioned above: precision of the techniques, tumor reduction, and the effects of these techniques on a neighboring artery.

3.1 Precision

Precision of HIFU and LITT were compared by multiple temperature profiles for each technique. Figure 3.1 (a) and (b) depict temperature profiles along the width of the tumor for both therapies. Since the transducer, in case of HIFU, was insonated for 1 s and then turned off, HIFU showed highest peak of rise in temperature at t = 1 s which gradually diminished over time. In case of LITT, the laser application was continuous and hence, rise in temperature increased over time. However, the point of difference between these two therapies lies in their ability to induce rise in temperature in a focally contained region i.e. tumor. Figure 3.1 (a) and (b) depicted HIFU therapy to be more radially focused compared to LITT. For HIFU, as the temperature rise peaked at ΔT = 14.264 K, the peak became slenderer and more focused. In LITT, however, as ΔT increased, the graph became wider at the base, depicting a considerable reduction in radial focus. Figure 3.2 (a) and (b) depict temperature profiles along the length of

the tumor for HIFU and LITT respectively. In Figure 3.2 (a), most of the heating occurred in the elliptical tumor region between 14.5 mm and 19.5 mm along the axis of the tumor. Heat was absorbed by the surrounding healthy tissue as well. A slight increase in temperature was observed below 10 mm. This was because the artery 1.5 mm below the tumor caused the side-lobe heating effect with pressure maxima lying outside the tumor region. In (b), LITT showed better focusing ability in the axial direction compared to its radial direction. Overall, HIFU was more focally-contained compared to LITT.

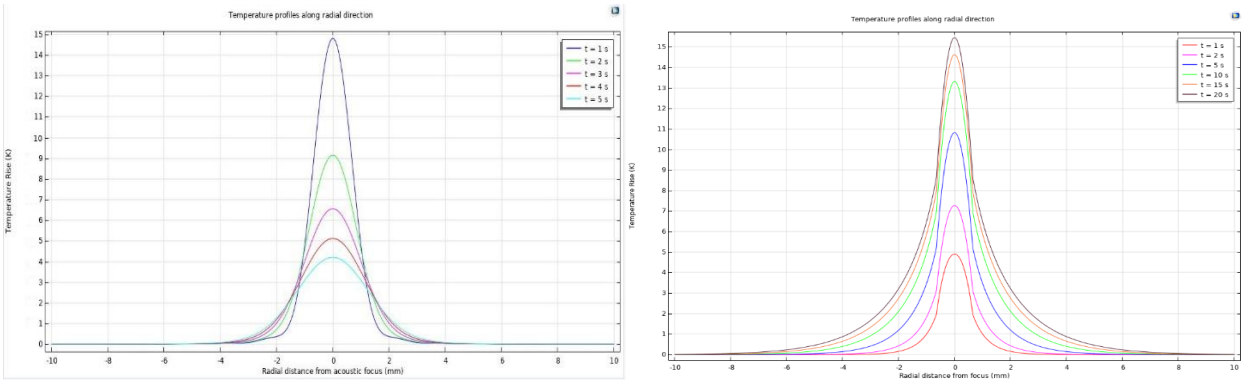

Fig. 3.1: Temperature profiles along radial direction of tumor (a) in case of HIFU and (b) in case of LITT.

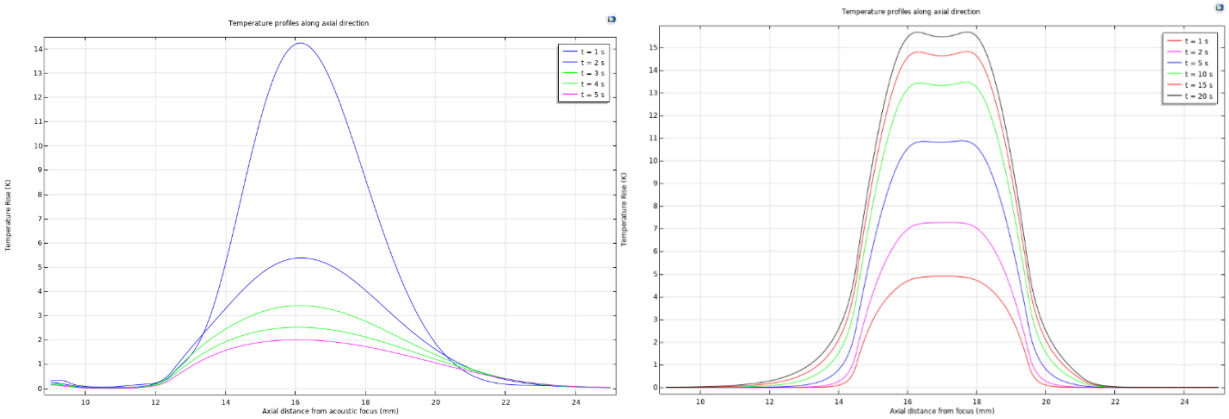

Fig. 3.2: Temperature profile in axial direction of tumor (a) in case of HIFU and (b) in case of LITT.

3.2 Degree of Tissue Damage

Figures 3.3 (a) and (b) and 3.4 (a) and (b) depict degree of tumor tissue injury along radial and axial directions in case of HIFU and LITT respectively. In figure 3.3 (a), most damage occurred to tumor tissue at the radial focus with a damage degree of approximate 0.0017. A

damage integral value of 1 signifies 63% cell necrosis volume [38]. Tumor tissue damage decreased gradually along the radial axis of the tumor. In figure 3.4 (b), most damage to the tumor occurred at the radial focus with a damage degree of 0.2924. Injury to tumor tissue decreased rather erratically along the radial axis of tumor in case of LITT. In figure 3.4 (a), least damage to the tissue was noticed at the farthest edge of the tumor. Damage was focused on the axial center of the tumor. The tumor edge close to the HIFU transducer showed considerable damage. In figure 3.4 (b), damage peak was maintained at the axial focus of the tumor. The degree of damage decreased gradually along the axial length of the tumor. The damage was maximum at the central region of the tumor. In general, LITT depicted a higher degree of tumor tissue injury as compared to HIFU.

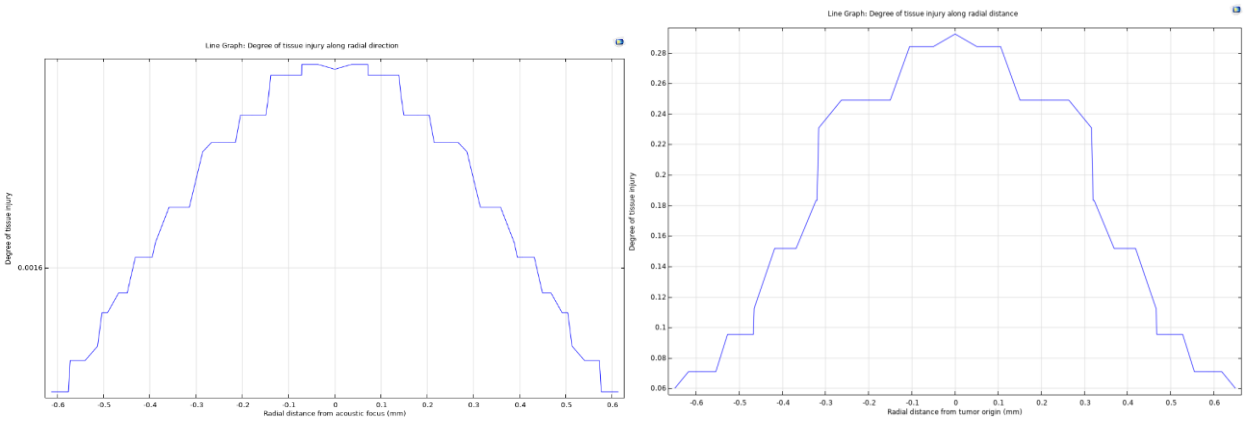

Fig. 3.3: Tumor reduction along radial direction (a) in case of HIFU and (b) in case of LITT

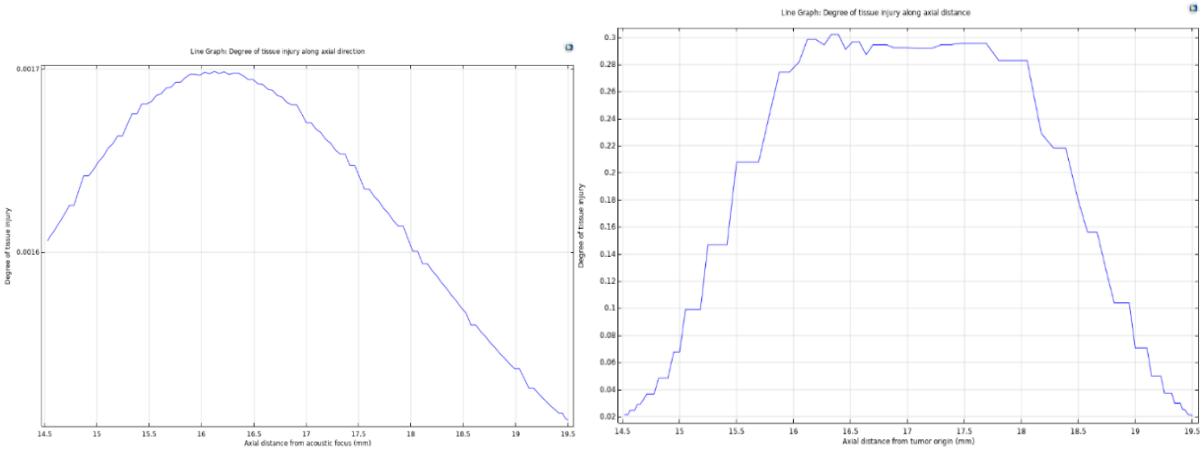

Fig. 3.4: Tumor reduction in axial direction (a) in case of HIFU and (b) in case of LITT

3.3 Effect on neighboring artery

Lastly, the effects of HIFU and LITT on neighboring artery were graphed in Figures 3.5 through 3.8. In Figure 3.5, the first case study was utilized wherein the artery lay in the path of the HIFU beam and at a distance of 1.5 mm from the tumor site. Tissue damage of 0.0015 was depicted in the arterial wall closer to the tumor site as contoured in (a).

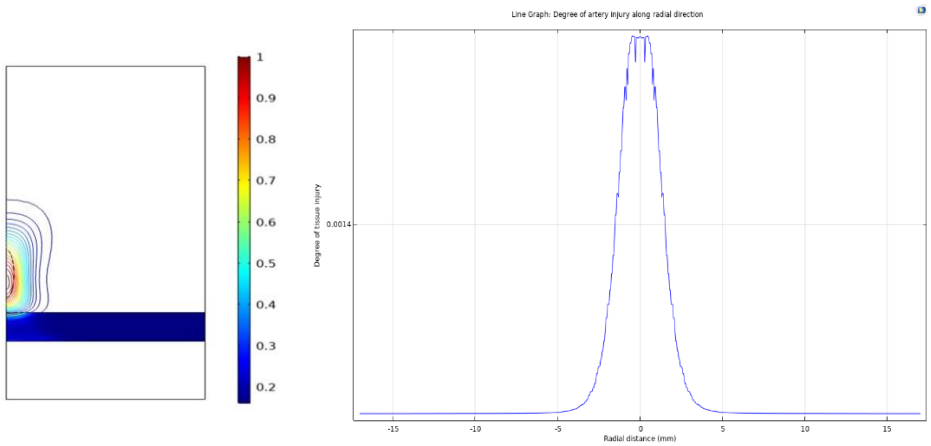

Fig. 3.5: Case Study I - Tissue damage in artery lying in the path of HIFU beam (a) 2D view (b) radial direction

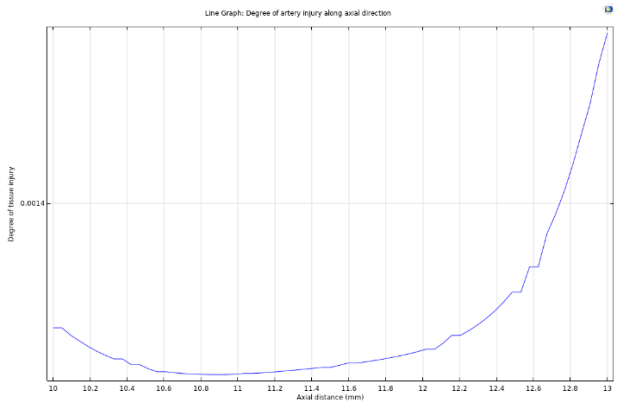

Fig. 3.5: Case Study I - Tissue damage in artery lying in the path of HIFU beam (c) axial direction

In Figure 3.6, the second case study was used wherein the artery lay away from the path of the HIFU beam and at a distance of 1.5 mm from the tumor site. Tissue damage trend was similar to that in case study I.

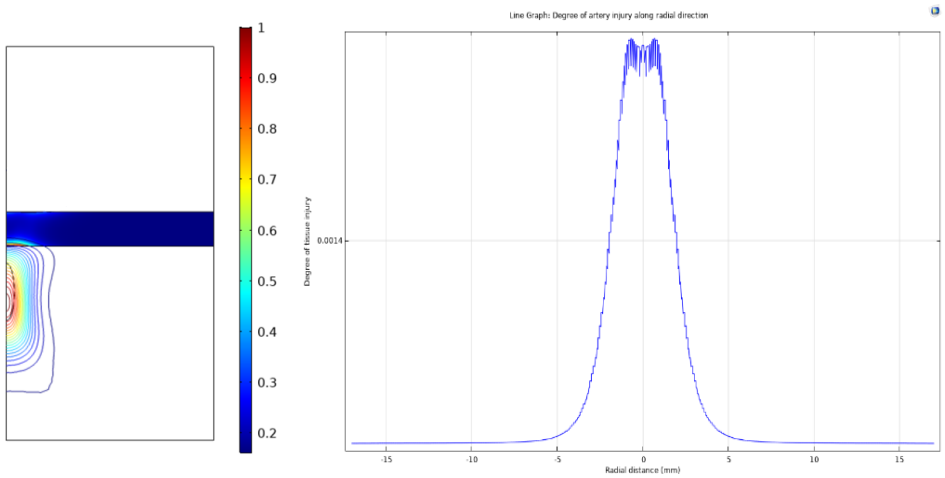

Fig. 3.6: Case Study II - Tissue damage in artery away from HIFU beam (a) 2D view (b) radial direction

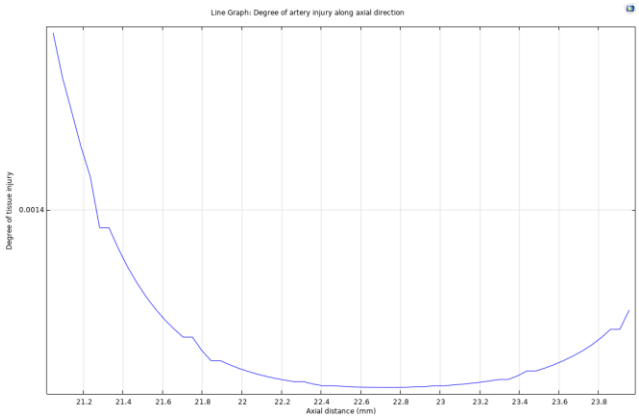

Fig. 3.6: Case Study II - Tissue damage in artery away from HIFU beam (c) axial direction

In Figure 3.7, the third case study was analyzed in which artery was placed 1.5 mm away from LITT focal region. Artery wall close to the tumor underwent tissue damage of 0.007 as shown in 2D contour in Figure 3.7 (a).

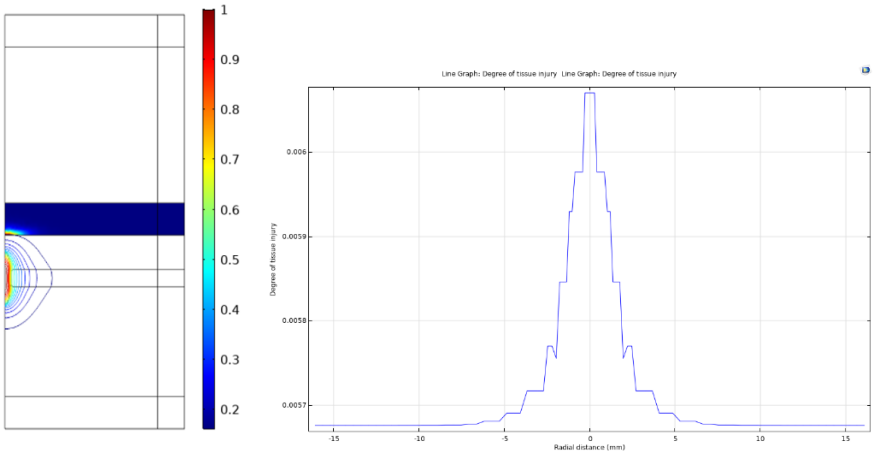

Fig. 3.7: Case Study III - Tissue damage in artery 1.5 mm away from LITT focus (a) 2D view (b) radial direction

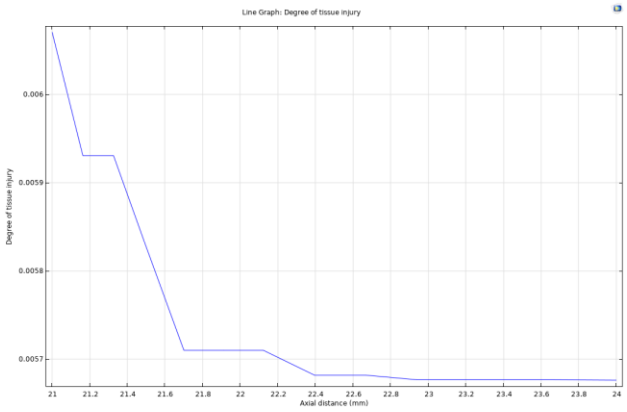

Fig. 3.7: Case Study III - Tissue damage in artery 1.5 mm away from LITT focus (c) axial direction

Figure 3.8 employed the last case study to test LITT environment wherein the artery lay at a distance of 3 mm from the tumor site. Damage integral of 0.0057 was shown in the arterial wall closer to the tumor site as contoured in Figure 3.8 (a).

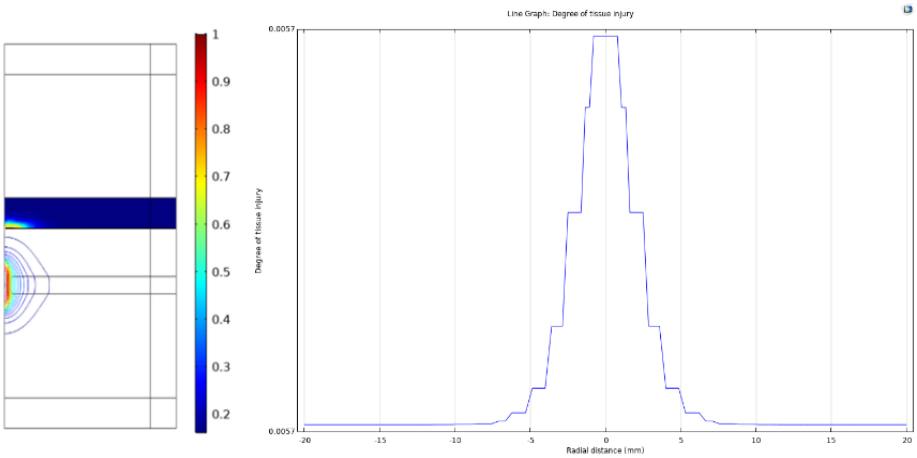

Fig. 3.8: Case Study IV - Tissue damage in artery 3 mm away from LITT focus (a) 2D view (b) radial direction

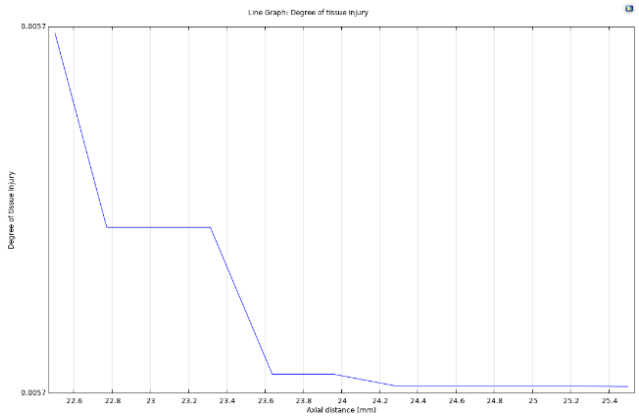

Fig. 3.8: Case Study IV - Tissue damage in artery 3 mm away from LITT focus (c) axial direction

It was observed in figures 3.5 and 3.8 that an organ in the path of the HIFU beam bore similar effects to one away from the beam but placed at the same distance from the tumor site. The determining factor for the effect of HIFU on a neighboring organ was the distance of the organ from the tumor site instead of its presence in the path or away from the beam. In case of LITT, its effect on the neighboring artery decreased by 1.23% over a distance of 1.5 mm.

3.4 Conclusions

The findings of this study allow the conclusion that HIFU is more focally contained compared to LITT. LITT caused more irreversible necrotic damage to the tumor site compared to

HIFU by 172%. Both the techniques resulted in thermal damage to neighboring artery, however the damage caused by HIFU was 4.67% less compared to that caused by LITT.

Table 2-1: Material properties of brain tissue [39, 40]

Material properties of brain tissue	**Value**
Density	1050 kg/m^3 [39]
Speed of sound	1562 m/s [40]
Thermal conductivity	0.537 W/ (m.°C) [39]
Heat capacity at constant pressure	3682 J/(kg.°C) [39]
Absorption coefficient	8.6 Np/m/MHz [40]

Table 2-2: Material properties of arterial blood [39, 40]

Material properties of arterial blood	**Value**
Density	1057 kg/m^3 [39]
Speed of sound	1584 m/s [40]
Thermal Conductivity	0.488 W/ (m.°C) [39]
Heat capacity at constant pressure	3651 J/(kg.°C) [39]
Blood perfusion rate	0.866 1/s [33]
Absorption coefficient	1.7 Np/m/MHz [40]

Table 2-3: Tissue properties used to compute fraction of necrotic tissue [33]

Arrhenius equation parameters	**Value**
Frequency factor A	7.39 x 10^{39} 1/s [33]
Activation energy ΔE	2.577 x 10^5 J/mol [33]
Polynomial order	1 [33]

REFERENCES

[1] P. de Robles *et al.*, "The worldwide incidence and prevalence of primary brain tumors: A systematic review and meta-analysis," *Neuro-Oncology*, vol. 17, no. 6. Oxford University Press, pp. 776–783, 2015, doi: 10.1093/neuonc/nou283.

[2] R. Arrangoiz, "Melanoma Review: Epidemiology, Risk Factors, Diagnosis and Staging," *Journal of Cancer Treatment and Research*, vol. 4, no. 1, p. 1, 2016, doi: 10.11648/j.jctr.20160401.11.

[3] M. M. Vargo, "Brain tumors and metastases," *Physical Medicine and Rehabilitation Clinics*, vol. 28, no. 1, pp. 115–141, 2017.

[4] J. MacDonell *et al.*, "Magnetic resonance-guided interstitial high-intensity focused ultrasound for brain tumor ablation," *Neurosurgical Focus*, vol. 44, no. 2, 2018, doi: 10.3171/2017.11.FOCUS17613.

[5] K. A. Yaeger and M. N. Nair, "Surgery for brain metastases," *Surg Neurol Int*, vol. 4, no. Suppl 4, pp. S203–S208, 2013.

[6] M. Mut, "Surgical treatment of brain metastasis: a review," *Clin Neurol Neurosurg*, vol. 114, pp. 1–8, 2012, doi: 10.1016/j.clineuro.2011.10.013.

[7] C. A. Graham and T. F. Cloughesy, "Brain tumor treatment: chemotherapy and other new developments," in *Seminars in oncology nursing*, 2004, vol. 20, no. 4, pp. 260–272.

[8] K. Hynynen, N. McDannold, G. Clement, F. A. Jolesz, E. Zadicario, and R. Killiany, "Pre-clinical testing of a phased array ultrasound system for MRI-guided noninvasive surgery of the brain—a primate study," *Eur J Radiol*, vol. 59, pp. 149–156, 2006, doi: 10.1016/j.ejrad.2006.04.007.

[9] R. Rampling, A. James, and V. Papanastassiou, "The present and future management of malignant brain tumours: surgery, radiotherapy, chemotherapy," *Journal of Neurology, Neurosurgery & Psychiatry*, vol. 75, no. suppl 2, p. ii24, Jun. 2004, doi: 10.1136/jnnp.2004.040535.

[10] M. Lara-Velazquez *et al.*, "Advances in brain tumor surgery for glioblastoma in adults," *Brain Sciences*, vol. 7, no. 12. MDPI AG, Dec. 20, 2017, doi: 10.3390/brainsci7120166.

[11] M. P. Mehta and D. Khuntia, "Current strategies in whole-brain radiation therapy for brain metastases," *Neurosurgery*, vol. 57, no. suppl_5, pp. S4-33, 2005.

[12] S. Angeli and T. Stylianopoulos, “Biphasic modeling of brain tumor biomechanics and response to radiation treatment,” *Journal of biomechanics*, vol. 49, no. 9, pp. 1524–1531, 2016.

[13] J. Gonzalez, A. J. Kumar, C. A. Conrad, and V. A. Levin, “Effect of bevacizumab on radiation necrosis of the brain,” *International Journal of Radiation Oncology* Biology* Physics*, vol. 67, no. 2, pp. 323–326, 2007.

[14] O. Cohen-Inbar, P. Melmer, C. C. Lee, Z. Xu, D. Schlesinger, and J. P. Sheehan, “Leukoencephalopathy in long term brain metastases survivors treated with radiosurgery,” *J Neurooncol*, vol. 126, pp. 289–298, 2016, doi: 10.1007/s11060-015-1962-3.

[15] A. J. Sawyer, J. M. Piepmeier, and W. M. Saltzman, “New methods for direct delivery of chemotherapy for treating brain tumors,” *The Yale journal of biology and medicine*, vol. 79, no. 3–4, pp. 141–152, Dec. 2006, [Online]. Available: https://pubmed.ncbi.nlm.nih.gov/17940624.

[16] T. Koga and N. Saito, “Efficacy and limitations of stereotactic radiosurgery in the treatment of glioblastoma,” *Neurologia medico-chirurgica*, vol. 52, no. 8, pp. 548–552, 2012.

[17] R. Medvid, A. Ruiz, R. J. Komotar, J. R. Jagid, M. E. Ivan, and R. M. Quencer, “Current applications of MRI-guided laser interstitial thermal therapy in the treatment of brain neoplasms and epilepsy: a radiologic and neurosurgical overview,” *AJNR Am J Neuroradiol*, vol. 36, pp. 1998–2006, 2015, doi: 10.3174/ajnr.A4362.

[18] E. Christian, C. Yu, and M. L. J. Apuzzo, “Focused ultrasound: relevant history and prospects for the addition of mechanical energy to the neurosurgical armamentarium,” *World Neurosurg*, vol. 82, pp. 354–365, 2014, doi: 10.1016/j.wneu.2014.06.021.

[19] W. J. Elias, D. Huss, T. Voss, J. Loomba, M. Khaled, and E. Zadicario, “A pilot study of focused ultrasound thalamotomy for essential tremor,” *N Engl J Med*, vol. 369, pp. 640–648, 2013, doi: 10.1056/NEJMoa1300962.

[20] C. Hoppe, J.-A. Witt, C. Helmstaedter, T. Gasser, H. Vatter, and C. E. Elger, “Laser interstitial thermotherapy (LiTT) in epilepsy surgery,” *Seizure*, vol. 48, pp. 45–52, 2017.

[21] E. Maloney and J. H. Hwang, “Emerging HIFU applications in cancer therapy,” *Int J Hyperthermia*, vol. 31, pp. 302–309, 2015, doi: 10.3109/02656736.2014.969789.

[22] M. G. Keane, K. Bramis, S. P. Pereira, and G. K. Fusai, “Systematic review of novel ablative methods in locally advanced pancreatic cancer,” *World J Gastroenterol*, vol. 20, pp. 2267–2278, 2014, doi: 10.3748/wjg.v20.i9.2267.

[23] F. Wolfram and T. G. Lesser, “A simulation study of the HIFU ablation process on lung tumours, showing consequences of atypical acoustic properties in flooded lung,” *Zeitschrift für Medizinische Physik*, vol. 29, no. 1, pp. 49–58, 2019.

[24] P. Smirnov and K. Hynynen, “Design of a HIFU array for the treatment of deep venous thrombosis: a simulation study,” *Physics in Medicine & Biology*, vol. 62, no. 15, pp. 6108–6125, 2017, doi: 10.1088/1361-6560/aa71fb.

[25] M. Almekkawy and E. S. Ebbini, “The Optimization of Transcostal Phased Array Refocusing Using the Semidefinite Relaxation Method,” *IEEE transactions on ultrasonics, ferroelectrics, and frequency control*, vol. 67, no. 2, pp. 318–328, 2019.

[26] D. McMahon and M. Almekkawy, “Elements Selection for Transcostal HIFU Refocusing Method: Simulation Study,” *IEEE Transactions on Ultrasonics, Ferroelectrics, and Frequency Control*, vol. 67, no. 7, pp. 1366–1376, 2020, doi: 10.1109/TUFFC.2020.2973678.

[27] Q. Tan, X. Zou, Y. Ding, X. Zhao, and S. Qian, “The influence of dynamic tissue properties on HIFU hyperthermia: A numerical simulation study,” *Applied Sciences (Switzerland)*, vol. 8, no. 10, Oct. 2018, doi: 10.3390/app8101933.

[28] D. S. Kwon, J. H. Sung, C. Y. Park, and J. S. Jeong, “Phase-inverted multifrequency HIFU transducer for lesion expansion: A simulation study,” *IEEE Transactions on Ultrasonics, Ferroelectrics, and Frequency Control*, vol. 65, no. 7, pp. 1125–1132, Jul. 2018, doi: 10.1109/TUFFC.2018.2830108.

[29] M. A. Solovchuk, T. W. H. Sheu, W. L. Lin, I. Kuo, and M. Thiriet, “Simulation study on acoustic streaming and convective cooling in blood vessels during a high-intensity focused ultrasound thermal ablation,” *International Journal of Heat and Mass Transfer*, vol. 55, no. 4, pp. 1261–1270, Jan. 2012, doi: 10.1016/j.ijheatmasstransfer.2011.09.023.

[30] M. A. Solovchuk, S. C. Hwang, H. Chang, M. Thiriet, and T. W. H. Sheu, “Temperature elevation by HIFU in ex vivo porcine muscle: MRI measurement and simulation study,” *Medical Physics*, vol. 41, no. 5, 2014, doi: 10.1118/1.4870965.

[31] S. Missios, K. Bekelis, and G. H. Barnett, “Renaissance of laser interstitial thermal ablation,” *Neurosurg Focus*, vol. 38, no. 3, p. E13, 2015, doi: 10.3171/2014.12.FOCUS14762.

[32] R. Medvid, A. Ruiz, R. J. Komotar, J. R. Jagid, M. E. Ivan, and R. M. Quencer, “Current applications of MRI-guided laser interstitial thermal therapy in the treatment of brain neoplasms

and epilepsy: a radiologic and neurosurgical overview," *AJNR Am J Neuroradiol*, vol. 36, pp. 1998–2006, 2015, doi: 10.3174/ajnr.A4362.

[33] M. Nour, M. Bougataya, and A. Lakhssassi, "Modeling the Laser Thermal Therapy in Treatment of Brain Tumors," *International Journal of Computer Theory and Engineering*, vol. 9, no. 4, pp. 313–317, 2017, doi: 10.7763/IJCTE.2017.V9.1159.

[34] N. v. Patel, K. Frenchu, and S. F. Danish, "Does the thermal damage estimate correlate with the magnetic resonance imaging-predicted ablation size after laser interstitial thermal therapy?," *Operative Neurosurgery*, vol. 15, no. 2, pp. 179–183, 2018, doi: 10.1093/ons/opx191.

[35] W. J. Jermakowicz *et al.*, "Ablation dynamics during laser interstitial thermal therapy for mesiotemporal epilepsy," *PLoS ONE*, vol. 13, no. 7, Jul. 2018, doi: 10.1371/journal.pone.0199190.

[36] P. Saccomandi *et al.*, "Theoretical analysis and experimental evaluation of laser-induced interstitial thermotherapy in ex vivo porcine pancreas," *IEEE Transactions on Biomedical Engineering*, vol. 59, no. 10, pp. 2958–2964, 2012, doi: 10.1109/TBME.2012.2210895.

[37] H. Wang *et al.*, "Brain temperature and its fundamental properties: a review for clinical neuroscientists," *Frontiers in neuroscience*, vol. 8, p. 307, 2014.

[38] I. A. Chang, "Considerations for thermal injury analysis for RF ablation devices," *The open biomedical engineering journal*, vol. 4, pp. 3–12, Feb. 2010, doi: 10.2174/1874120701004020003.

[39] R. L. Mcintosh and V. Anderson, "A comprehensive tissue properties database provided for the thermal assessment of a human at rest," *Biophysical Reviews and Letters*, vol. 5, no. 03, pp. 129–151, 2010.

[40] A. Kyriakou, "Multi-Physics Computational Modeling of Focused Ultrasound Therapies," ETH Zurich, 2015.

Investigation of Ablation techniques for different types of brain tumors

ORIGINALITY REPORT

6%	4%	4%	2%
SIMILARITY INDEX	INTERNET SOURCES	PUBLICATIONS	STUDENT PAPERS

PRIMARY SOURCES

1	thejns.org Internet Source	2%
2	Submitted to Higher Education Commission Pakistan Student Paper	1%
3	www.ess.washington.edu Internet Source	1%
4	M. F. J. Cepeda. "Microcoaxial Double Slot Antenna for Interstitial Hyperthermia: Design, Modeling and Validation", 2008 International Conference on Advances in Electronics and Micro-electronics, 09/2008 Publication	<1%
5	Abhijit Paul, Anup Paul. "Thermo-mechanical assessment of nanoparticle mixed vascular tissues under pulsed ultrasound and laser heating", International Journal of Thermal Sciences, 2021 Publication	<1%
6	Qiaolai Tan, Xiao Zou, Yajun Ding, Xinmin Zhao, Shengyou Qian. "The Influence of Dynamic Tissue Properties on HIFU Hyperthermia: A Numerical Simulation Study", Applied Sciences, 2018 Publication	<1%